*electronics*

MDPI

*Article*

# Puiseux-Type Resolution Expansion of the Settling-Time Expression for an *N*-Bit PWM DAC with a First-Order RC Filter

**Predrag Petronijević [1,2,*], Danilo Đokić [1] and Vladimir Rajović [1]**

[1] School of Electrical Engineering, University of Belgrade, Bulevar Kralja Aleksandra 73, 11120 Belgrade, Serbia; djokicd@etf.bg.ac.rs (D.Đ.); rajo@etf.bg.ac.rs (V.R.)
[2] Vlatacom Institute of High Technologies, Milutina Milankovića 5, 11070 Belgrade, Serbia
* Correspondence: predrag.petronijevic@vlatacom.com

**Abstract**

A pulse-width-modulated (PWM) output followed by a first-order resistor–capacitor (RC) filter provides a low-cost approach to digital-to-analog conversion. This paper develops a resolution expansion of a reference expression for the continuous rising-transition settling count in the parameter $\delta = 2^{-N}$, retaining the tolerance $\varepsilon$ exactly. Here $N$ denotes the resolution, and $\varepsilon$ is expressed as a fraction of one least significant bit. The coefficients contain half-integer powers of $\varepsilon$ and therefore have a Puiseux-type form. The first-order expression removes the exponential quotient of the reference expression and makes the dependence on $N$ and $\varepsilon$ explicit. Two higher-order truncations are also derived. For $1/8 \leq \varepsilon < 1/2$, the first and second truncations are proved never to underestimate the reference count. Both coincide with it at $\varepsilon = 1/8$. Over 1122 combinations with $N = 4$–$20$ and $\varepsilon = 0.125$–$0.45$, the maximum errors relative to the reference count are 0.21, 0.050, and 0.0025 PWM periods, with rounded-count agreement of 89.66%, 99.82%, and 100%, respectively. At every tested combination, the reference expression and the exact first-order model give the same rounded rising-transition count, and adding one period to each rounded truncated count covers the exact worst-case count over both transition directions. Both results are numerical and are established only for the tested grid.

**Keywords:** PWM DAC; settling time; RC filter; Puiseux-type expansion; resolution expansion; closed-form approximation

## 1. Introduction

A pulse-width-modulated (PWM) output followed by a passive low-pass filter is one of the simplest and lowest-cost approaches to digital-to-analog conversion in embedded systems, and its design is set by two opposing requirements of small ripple and short settling time. Conventional guidance estimates accuracy from the mean output voltage and the ripple amplitude and is valid only when the filter time constant is much larger than the PWM period [1].

An analytical time-domain treatment of the first-order case was given in [1], where code-dependent safe and forbidden operating zones were introduced so that the entire output waveform, and not only its mean value, must remain within a tolerance band around the target digital code. The analysis in [1] derived the worst-case number of PWM periods required for settling and showed, for an 8-bit converter with tolerance $\varepsilon = 1/4$, that 823 periods are needed rather than the 355 obtained from the conventional estimate. The results reported in [1] were validated numerically, by transient circuit simulation and by

Check for updates

Academic Editor: Andrea Ballo

Received: 23 September 2026
Revised: 20 October 2026
Accepted: 20 October 2026
Published: 23 October 2026

**Copyright:** © 2026 by the authors. Licensee MDPI, Basel, Switzerland. This article is an open access article distributed under the terms and conditions of the Creative Commons Attribution (CC BY) license.

measurements on a microcontroller-based prototype. Earlier time-domain results for the same converter were reported in [2].

Previous studies have considered PWM-based digital-to-analog conversion in terms of modulation methods, filter design, and implementation. Conventional PWM, pulse-count modulation, and first-order noise-shaping DACs were compared in [3]. A DSP-based PWM DAC and its low-pass-filter design were considered in [4], duty-cycle modulation techniques were reviewed in [5], and a pulse-width-adding DAC followed by low-pass filtering was proposed in [6]. The code-transition settling criterion of [1], in which the filtered output signal must remain within the admissible interval around the target code, is not considered in these works.

Closed-form estimates of transient duration have long been used in circuit design. The Elmore delay of RC trees was shown in [7] to be an upper bound on the 50% delay, and the settling time of operational amplifiers was treated analytically in [8]. Such results are examples of design-oriented analysis [9], in which the form of the expression shows which parameter controls the response. The present study applies this design-oriented approach to the PWM DAC settling criterion derived in [1].

The method is an asymptotic expansion. A function is approximated by the leading terms of an expansion in a small parameter, and the neglected remainder is estimated or bounded [10]. In the model of [1], the target code with the longest settling time is determined by a transcendental equation. Equations of this type can be solved in closed form with the Lambert W function [11]. Numerical methods provide an alternative when a compact analytical expression is unavailable. In filter design they include constrained numerical optimization. An example is the software of [12], which is based on a genetic algorithm and was tested on the design of a two-dimensional recursive filter. Numerical evaluation is used here for the exact first-order model, with which the expansion is compared.

The present work focuses on the analytical form of the settling criterion derived in [1]. The converter model and settling criterion of [1] are retained without modification, and a resolution expansion of the rising-transition count is developed while the tolerance $\varepsilon$ is retained without approximation. This gives a closed-form first-order expression and two higher-order truncations whose errors are evaluated before and after rounding to an integer number of PWM periods. The reference rising-transition expression contains the quotient

$$\frac{e^{\varepsilon/2^{N-3}}-1}{e^{\sqrt{2\varepsilon}/2^{N-1}}-1}, \tag{1}$$

in which the numerator argument is of order $\varepsilon$ while the denominator argument is of order $\sqrt{\varepsilon}$. The resulting expansion contains coefficients with half-integer powers of $\varepsilon$ and therefore has a Puiseux-type form [13,14]. The term Puiseux-type refers to the coefficients, because the expansion itself is an ordinary power series in $\delta = 2^{-N}$ with integer exponents and the fractional powers appear only in its coefficients, which are polynomials in $\sqrt{2\varepsilon}$. A Puiseux series in $\varepsilon$ in the strict sense would be obtained by expanding the quotient in powers of $\sqrt{2\varepsilon}$ for fixed $N$. Because of this quotient, the reference expression does not show how the required number of periods depends on $N$ and $\varepsilon$ separately. The expansion removes the quotient.

## 2. Reference Criterion and Notation

The converter resolution in bits is denoted by $N$, and the admissible tolerance, expressed as a fraction of one least significant bit (LSB), by $\varepsilon$. The safe zones of [1] are defined for $0 \leq \varepsilon < 1/2$, and at $\varepsilon = 1/2$ the boundaries of the safe zones for adjacent codes meet, so no forbidden zones remain. Although $\varepsilon = 0$ is included in the safe-zone definition, the

reference settling-time expression, Equation (69) of [1], is not defined at this point because direct substitution gives undefined terms. The tolerance is therefore taken from the open interval $0 < \varepsilon < 1/2$, and the analysis is further restricted to $1/8 \leq \varepsilon < 1/2$.

The normalized filter parameter defined by Equation (35) of [1] is

$$k = \frac{\varepsilon}{2^{N-3}}. \tag{2}$$

Here $k = T/(RC)$ is the ratio of the PWM period $T$ to the time constant of the filter. Equation (2) gives its design value, so that a prescribed tolerance $\varepsilon$ corresponds to $RC = 2^{N-3}T/\varepsilon$. This value of $k$ is slightly smaller than the exact limit given by Equation (36) of [1], satisfies the safe-zone condition for every code, and is the nominal value used in the circuit simulations of [1].

For a transition from code $d_1 = 0$, Equation (68) of [1] gives the following approximation to the position of the settling-time maximum:

$$d_{2,\max 1} = \sqrt{\frac{2^N}{k}} = \sqrt{\frac{2^N}{\frac{\varepsilon}{2^{N-3}}}} = \frac{2^{N-1}}{\sqrt{2\varepsilon}}. \tag{3}$$

The position given by Equation (3) is obtained in [1] from the stationarity condition of the rising-transition count and is in general not an integer. It lies within the code range only if $d_{2,\max 1} \leq 2^N - 1$, which is equivalent to $\varepsilon \geq 1/\left[8\left(1 - 2^{-N}\right)^2\right]$. This limit equals 0.142 for $N = 4$ and 0.126 for $N = 8$, and it tends to $1/8$ from above as $N$ increases. For $\varepsilon < 1/8$ the position therefore lies above the code range for every $N$. The rising-transition count then increases with the target code over the whole code range, and the worst-case rising transition is the one to the highest code $2^N - 1$. In that case Equation (69) of [1] overestimates the exact rising-transition count. The operating points of [1], for which $\varepsilon = 1/3$, $1/4$, and $1/5$, are not affected.

Because of this overestimate, the results are given for $1/8 \leq \varepsilon < 1/2$, which is referred to below as the considered range. For the few combinations of $N$ and $\varepsilon$ in this range at which $\varepsilon$ is below the limit $1/\left[8\left(1 - 2^{-N}\right)^2\right]$, the position given by Equation (3) remains above the highest code. At the tested combinations for which this occurs, the reference count differs from the exact rising-transition count by less than 0.09 PWM periods.

The number of PWM periods after which the entire output waveform enters and permanently remains within the code-decision interval of $\pm\frac{1}{2}$LSB around the target code, evaluated at the position given by Equation (3), is given by Equation (69) of [1], which can be written as

$$\nu_{ref}(N, \varepsilon) = -\frac{1}{k} \ln \Lambda(N, \varepsilon), \tag{4}$$

where

$$\Lambda(N,\ \varepsilon) = 1 - \frac{1}{2}\left(\frac{1}{\sqrt{2\varepsilon}} - 2^{-N}\right)\frac{e^{\varepsilon/2^{N-3}} - 1}{e^{\sqrt{2\varepsilon}/2^{N-1}} - 1} \tag{5}$$

is the expression appearing inside the logarithm of Equations (69) and (81) of [1].

In this paper, $\nu_{ref}$ denotes the reference count before rounding, against which all approximations are compared. Its value rounded up to the next integer, $n_{ref} = \lceil \nu_{ref} \rceil$, is the rounded reference count used in the comparisons below.

In [1], the approximation used to obtain Equation (69) was compared with the corresponding exact rising-mode expression for $\varepsilon = 1/3$, $1/4$, and $1/5$. The differences between the continuous counts were negligible, and the rounded counts coincided for all cases included in the comparison given in [1]. The reference count $\nu_{ref}$ is nevertheless based on the approximations introduced in [1] for the parameter $k$ and for the position of the settling-time maximum $d_{2,\max 1}$. The errors reported in Sections 5.1–5.3 are therefore mea-

sured relative to $\nu_{ref}$, not to the exact rising-transition count of the first-order RC model. The exact rising-transition count $\nu_{ex}$, referred to below as the exact count, is defined as the maximum of the exact rising-mode expression, Equation (65) of [1], over the integer target codes $d_2 = 1, \ldots, 2^N - 1$. It is obtained without the approximation of Equation (3), with $k$ fixed at its design value given by Equation (2). Its rounded value is $n_{ex} = \lceil \nu_{ex} \rceil$. The exact count is compared with $\nu_{ref}$ in Section 5.4.

The present analysis considers only the rising code transition because its expression is suitable for the resolution expansion developed in Section 3. In [1], the decreasing transition was identified as the conservative worst case. Equation (80) of [1] expresses the corresponding integer design count as one PWM period more than the rounded rising-transition count. This one-period correction is therefore applied after the rising-transition count is obtained. Any additional error introduced by truncating the expansion is considered separately in Sections 4.4 and 5.

## 3. Puiseux-Type Resolution Expansion

The converter resolution $N$ appears in Equation (5) only through the quantity $2^{-N}$, which is small over the resolution range considered here: it equals $1/16$ at four bits and falls below $10^{-6}$ at twenty bits. We therefore use $\delta$ as the expansion parameter. No expansion is made in $\varepsilon$, which is retained exactly. Accordingly, we set

$$\delta = 2^{-N}, \quad s = \sqrt{2\varepsilon}, \tag{6}$$

so that $\delta$ carries the resolution dependence and is the small parameter, while $s$ depends only on $\varepsilon$. The variable $s$ is introduced because Equation (5) contains both $\varepsilon$ and $\sqrt{2\varepsilon}$, and in terms of $s$ the coefficients of the expansion are polynomials. Equation (6) is a change in variables, and $\delta$ and $s$ are not additional settings of the converter or of the filter. The considered range corresponds to $1/2 \le s < 1$. At fixed $\varepsilon$, each additional retained power of $\delta$ improves the asymptotic error order by one power of $2^{-N}$. With this notation, the two exponential arguments in Equation (5) become

$$a = \frac{\varepsilon}{2^{N-3}} = 4s^2\delta, \quad b = \frac{\sqrt{2\varepsilon}}{2^{N-1}} = 2s\delta, \quad \frac{a}{b} = 2s. \tag{7}$$

Both arguments tend to zero as $\delta \to 0$, so the numerator and denominator of the exponential quotient in Equation (1) approach zero at the same time. The quotient therefore has the indeterminate form $0/0$ at $\delta = 0$, which makes Equation (5) inconvenient for direct expansion.

To remove the $0/0$ indeterminate form, we introduce the function

$$\varphi(x) = \frac{e^x - 1}{x}, \; x \neq 0, \; \varphi(0) = 1 \tag{8}$$

which is analytic everywhere. Since Equation (8) can be rewritten as $e^x - 1 = x\varphi(x)$, the exponential quotient becomes

$$\frac{e^a - 1}{e^b - 1} = \frac{a}{b} \cdot \frac{\varphi(a)}{\varphi(b)} = 2s\rho, \; \rho = \frac{\varphi(a)}{\varphi(b)}, \tag{9}$$

where the ratio $\rho$ is analytic in $\delta$ at the origin and $\rho \to 1$ as $\delta \to 0$. The square root in $s = \sqrt{2\varepsilon}$ comes from the approximate position of the settling-time maximum in Equation (3). The expansion is therefore an ordinary power series in $\delta$, while its coefficients contain fractional powers of $\varepsilon$, which gives the expansion its Puiseux-type form.

Using the definitions in Equation (6), the algebraic prefactor multiplying the exponential quotient in Equation (5) can be rewritten as

$$\frac{1}{2}\left(\frac{1}{\sqrt{2\varepsilon}} - 2^{-N}\right) = \frac{1 - s\delta}{2s}. \tag{10}$$

Multiplying this prefactor by the exponential quotient $2s\rho$ from Equation (9) cancels the factor $2s$ and gives

$$\Lambda = 1 - (1 - s\delta)\rho. \tag{11}$$

Since $\varphi(x) > 0$ for all $x \in \mathbb{R}$, the function ln(φ(x)) is analytic at $x = 0$ and has the Taylor expansion

$$\ln(\varphi(x)) = \frac{x}{2} + \frac{x^2}{24} - \frac{x^4}{2880} + \cdots. \tag{12}$$

Using Equation (12) gives

$$\ln(\varphi(a)) - \ln(\varphi(b)) = \frac{a - b}{2} + \frac{a^2 - b^2}{24} + \cdots. \tag{13}$$

By Equation (7) both $a$ and $b$ are proportional to $\delta$. The first term on the right-hand side of Equation (13) is therefore proportional to $\delta$, while the second is proportional to $\delta^2$. All terms after the first are of order $\delta^2$ or higher and can be included in $O(\delta^2)$, where $O(\delta^2)$ denotes a quantity bounded by a constant multiple of $\delta^2$ as $\delta \to 0$. Expanding the exponential then gives $\rho = 1 + (a - b)/2 + O(\delta^2)$. Substituting this result into Equation (11) gives

$$\Lambda = s\delta - \frac{a - b}{2} + O(\delta^2) = 2s(1 - s)\delta + O(\delta^2). \tag{14}$$

Equation (14) shows that $\Lambda$ is linear in $\delta$ to leading order. Its coefficient is a polynomial in $s = \sqrt{2\varepsilon}$, so it contains half-integer powers of $\varepsilon$ and is not analytic at $\varepsilon = 0$. Retaining terms through $\delta^3$ in the expansion of Equation (11) gives

$$\Lambda = A_1\delta + A_2\delta^2 + A_3\delta^3 + O(\delta^4), \tag{15}$$

with

$$A_1 = 2s(1 - s), \tag{16}$$

$$A_2 = \frac{4}{3}s^2(1 - s)(2s - 1), \tag{17}$$

$$A_3 = -\frac{1}{3}s^3(2s - 1)(4s^2 - 6s + 1). \tag{18}$$

The factor $(1 - s)$ in $A_1$ and $A_2$ is zero at $s = 1$, corresponding to $\varepsilon = 1/2$, the upper limit of the considered range. The coefficient $A_3$ is not zero there, so that close to this limit the third-order term is no longer small compared with the first two. The factor $(2s - 1)$, common to $A_2$ and $A_3$, is zero at $s = 1/2$, corresponding to $\varepsilon = 1/8$.

## 4. Simplified Design Formula and Truncation Error

The expansion in Equation (15) is truncated to obtain a simplified design formula and two higher-order approximations, and their leading errors are derived.

### *4.1. Truncations and Leading Errors*

The first-order, second-order, and third-order truncations of $\Lambda$ are

$$\Lambda_1 = A_1\delta, \quad \Lambda_2 = A_1\delta + A_2\delta^2, \quad \Lambda_3 = A_1\delta + A_2\delta^2 + A_3\delta^3. \tag{19}$$

For $m = 1, 2, 3$, the corresponding continuous settling count is $\nu_m = -(1/k)\ln\Lambda_m$, and the rounded count is $n_m = \lceil \nu_m \rceil$. The criterion based on $\Lambda_m$ is denoted by $P_m$, so $P_1$, $P_2$, and $P_3$ are the first-order, second-order, and third-order criteria in $\delta$. $P_1$ reduces to the closed-form expression in Equation (20).

Substituting $\Lambda_1$ into $\nu_1$ and simplifying the logarithmic terms gives the following closed-form approximation for the continuous rising-transition settling count:

$$\nu_1 = \frac{2^{N-3}}{\varepsilon}\left[(N-1)\ln 2 - \ln\left(\sqrt{2\varepsilon}\left(1-\sqrt{2\varepsilon}\right)\right)\right]. \tag{20}$$

Equation (20) gives a closed-form approximation of the continuous rising-transition settling count defined by Equation (4). The exponential terms are removed, and the dependence on the resolution $N$ and the tolerance $\varepsilon$ is shown explicitly. For a fixed tolerance $\varepsilon$, the expression directly shows how the required number of PWM periods changes with the converter resolution $N$.

The corresponding approximate integer rising-transition count is $n_1 = \lceil \nu_1 \rceil$. $P_2$ and $P_3$ provide higher-order approximations by including one and two additional algebraic terms, respectively. The effect of truncation on the rounded count is evaluated in Section 5.

To determine the error of $P_1$, the reference count $\nu_{ref}$ is compared with the first-order approximation $\nu_1$. Writing $\Lambda = \Lambda_1(1 + (A_2/A_1)\delta + O(\delta^2))$ and substituting this form into Equation (4), followed by expansion of the logarithm, gives

$$\nu_1 - \nu_{ref} = \frac{2s-1}{6s} + O(\delta). \tag{21}$$

Equation (21) shows that the leading error of $P_1$ depends only on the tolerance $\varepsilon$ and not on the resolution $N$.

Repeating the same comparison for the second-order approximation gives the leading error of $P_2$,

$$\nu_2 - \nu_{ref} = -\frac{(2s-1)\left(4s^2-6s+1\right)}{24(1-s)}\delta + O(\delta^2). \tag{22}$$

Including the third-order term gives

$$\nu_3 - \nu_{ref} = O(\delta^2). \tag{23}$$

Since $\delta = 2^{-N}$, the terms $O(\delta)$ and $O(\delta^2)$ correspond to $O(2^{-N})$ and $O(4^{-N})$. The leading error of $P_1$ is therefore independent of $N$, while the leading errors of $P_2$ and $P_3$ decrease with increasing resolution as $2^{-N}$ and $4^{-N}$, respectively.

For $0 < \varepsilon < 1/2$, $s$ lies between 0 and 1. The leading error in Equation (21) therefore has the sign of $(2s - 1)$ and becomes zero at $s = 1/2$, corresponding to $\varepsilon = 1/8$. To examine this point directly in the original expression, substituting $s = 1/2$ into $a$ and $b$ from Equation (7) gives

$$a = 4s^2\delta = \delta, \quad b = 2s\delta = \delta, \tag{24}$$

so that $a = b$, and the ratio $\rho = \varphi(a)/\varphi(b)$ equals one for every $\delta$. Substituting $\rho = 1$ into Equation (11) gives

$$\Lambda = 1 - (1 - s\delta)\rho = s\delta = \frac{\delta}{2} = 2s(1-s)\delta = \Lambda_1. \tag{25}$$

At $\varepsilon = 1/8$, Equation (25) gives $\nu_1 = \nu_{ref}$ for every resolution $N$. For $\varepsilon > 1/8$, the leading error in Equation (21) is positive. It is shown in Section 4.4 that the full error $\nu_1 - \nu_{ref}$ is non-negative for all $1/8 \leq \varepsilon < 1/2$.

*4.2. Interpretation and Practical Scope of Equation (20)*

Since $(N-1)\ln 2 - \ln(s(1-s)) = (N+1)\ln 2 - \ln(4s(1-s))$, Equation (20) can be written as

$$\nu_1 = \frac{1}{k}\left[(N+1)\ln 2 + \ln\frac{1}{4s(1-s)}\right], \quad s = \sqrt{2^{N-2}k}, \tag{26}$$

where $k = T/(RC)$, and the second relation follows from Equations (2) and (6). The first term, $(N+1)\ln 2/k$, is the number of periods after which the response of an RC filter to a full-scale step is within $\frac{1}{2}$LSB of its final value. The second term is a correction to this count that is zero for $s = 1/2$ and positive for $1/2 < s < 1$.

The settling criterion of [1] requires the entire output waveform to enter and remain within the code-decision interval of $\pm\frac{1}{2}$LSB, and the tolerance $\varepsilon$ appears in the reference expression only through the filter parameter $k$ of Equation (2). For an arbitrary combination of $R$, $C$, and PWM period $T$, the parameter $k = T/(RC)$ is therefore evaluated first. The quantity $\varepsilon = 2^{N-3}k$ is then the equivalent tolerance, that is, the tolerance for which Equation (2) gives the same filter. The steady-state ripple of this filter is largest at the code $2^{N-1}$, where its peak-to-peak value is approximately $2^N k/4 = 2\varepsilon$ LSB, which is the width of the safe zone of [1]. A prescribed tolerance is met if the equivalent tolerance does not exceed it. Equations (20) and (26) can be used if the equivalent tolerance lies in the considered range, $1/8 \le 2^{N-3}k < 1/2$, which is equivalent to

$$2^{N-2} < \frac{RC}{T} \le 2^N. \tag{27}$$

For $RC/T > 2^N$ the equivalent tolerance is below $1/8$ and lies outside the considered range, and the worst-case rising transition is then the one to the highest code. At $RC/T = 2^{N-2}$ the largest peak-to-peak ripple reaches approximately one LSB, and filters with $RC/T$ near or below this value must be assessed with the exact first-order model. Within the range of Equation (27), Equation (20) can be used for any first-order RC filter, but its accuracy decreases near the lower end of this range. This expression approximates the rising-transition reference count $\nu_{ref}$ under the settling criterion of [1]. The decreasing transition is covered by the one-period correction of [1].

*4.3. Behavior near the Limits of the Tolerance Range*

Equations (21)–(23) are asymptotic statements for $\delta \to 0$ at a fixed tolerance, and the neglected terms grow as $\varepsilon$ approaches the upper limit $\varepsilon = 1/2$. The reason is seen in Equations (16)–(18), where the coefficients $A_1$ and $A_2$ contain the factor $(1-s)$ and vanish at $s = 1$, while $A_3 = 1/3$ there. The truncations $\Lambda_1$ and $\Lambda_2$ are therefore close to $\Lambda$ only while $A_3\delta^3$ is small compared with $A_1\delta$, and close to the upper limit this requirement becomes

$$\frac{\delta^2}{6(1-s)} \ll 1. \tag{28}$$

Retaining one more term in Equation (21) gives

$$\nu_1 - \nu_{ref} = \frac{2s-1}{6s} + \frac{(2s-1)\left(1+6s-4s^2\right)}{72(1-s)}\delta + O(\delta^2). \tag{29}$$

The coefficients of $\delta$ in Equations (22) and (29) grow as $1/(1-s)$. As $\varepsilon \to 1/2$ at fixed $N$, Equation (15) gives $\Lambda \to \delta^3/3 + O(\delta^4)$, which is positive, so the reference count remains finite. In the same limit, $\Lambda_1$ and $\Lambda_2$ tend to zero in proportion to $(1-s)$, so that $\nu_1$ and $\nu_2$ increase as the logarithm of $1/(1-s)$ and both truncations overestimate the reference count. For $P_1$ the overestimate is $\nu_1 - \nu_{ref} = (1/k)\ln(\Lambda/\Lambda_1)$, which equals one PWM period when

$\Lambda/\Lambda_1 = e^k$, and for $P_2$ the same holds with $\Lambda_2$. Since $k \approx 4\delta$ near $\varepsilon = 1/2$, Equations (15)–(19) show that this occurs at a distance from the upper limit of approximately

$$\frac{1}{2} - \varepsilon \approx \frac{2^{-N}}{20} \text{ for } P_1, \qquad \frac{1}{2} - \varepsilon \approx \frac{2^{-N}}{24} \text{ for } P_2. \tag{30}$$

This distance is approximately 0.003 for $N = 4$ and 0.0002 for $N = 8$. Equation (30) is an asymptotic estimate and does not give a strict bound. The error of $P_3$, which retains the term $A_3\delta^3$, remains bounded up to the limit, where $\nu_3 - \nu_{ref}$ tends to approximately $1/4$ of a period.

Below $\varepsilon = 1/8$ the expansion in $\delta$ remains valid for a fixed tolerance. The leading error of $P_1$ in Equation (21) is then negative and increases in magnitude as the tolerance decreases, and the reference expression overestimates the exact rising-transition count.

### *4.4. Sign of the Truncation Error and Design Count*

At every tested combination in the considered range, none of the truncations lies below the reference count. For $P_1$ and $P_2$ this can be proved for every resolution.

**Proposition.** *Let* $1/8 \le \varepsilon < 1/2$ *and* $\delta > 0$. *Then*

$$\Lambda_1 \le \Lambda_2 \le \Lambda, \qquad \nu_{ref} \le \nu_2 \le \nu_1, \qquad n_{ref} \le n_2 \le n_1, \tag{31}$$

*with equality in the first two relations if and only if* $\varepsilon = 1/8$.

**Proof.** By Equation (17), $A_2 \ge 0$ for $1/2 \le s < 1$, so that Equation (19) gives $\Lambda_2 - \Lambda_1 = A_2\delta^2 \ge 0$, with equality only for $s = 1/2$. It therefore remains to show that $\Lambda \ge \Lambda_2$. Let $r = 2s$ and $x = 2s\delta$, so that $1 \le r < 2$ and $x > 0$. The arguments in Equation (7) are then $a = rx$ and $b = x$. In these variables, Equations (8), (9) and (11) give $\Lambda = 1 - (1 - x/2)(e^{rx} - 1)/[r(e^x - 1)]$, and Equations (16), (17) and (19) give $\Lambda_2 = (1 - r/2)x[1 + (r - 1)x/3]$. Multiplying $\Lambda - \Lambda_2$ by the positive quantity $r(e^x - 1)$, replacing the exponential functions by their power series, $e^x = \sum_{n=0}^{\infty} x^n/n!$ and $e^{rx} = \sum_{n=0}^{\infty} r^n x^n/n!$, and collecting the terms with the same power of $x$ gives

$$r(e^x - 1)(\Lambda - \Lambda_2) = r(r-1)\sum_{n=4}^{\infty} c_n(r)\frac{x^n}{n!}, \tag{32}$$

with

$$c_n(r) = n - 1 + \frac{n-2}{2}\left(r + r^2 + \cdots + r^{n-3}\right) - r^{n-2} - \frac{n(n-1)(2-r)}{6}. \tag{33}$$

The terms with $x$, $x^2$, and $x^3$ cancel, so that the sum in Equation (32) starts at $n = 4$. The coefficients $c_n(r)$ are positive for $1 \le r \le 2$. For $n = 4$, $c_4 = 1 + (r - 1)(2 - r) \ge 1$. For $n = 5$, the second derivative of $c_5$ with respect to $r$ is $3 - 6r < 0$, so that $c_5$ is concave on this interval and takes its smallest value at one of the end points, where it equals $8/3$ at $r = 1$ and 5 at $r = 2$. For $n \ge 6$, the two terms of Equation (33) with the highest powers of $r$ satisfy $\frac{n-2}{2}r^{n-3} - r^{n-2} = r^{n-3}\left(\frac{n-2}{2} - r\right) \ge 0$, because $(n - 2)/2 \ge 2$. Each of the remaining $n - 4$ powers of $r$ is at least one, and $2 - r \le 1$, so that $c_n(r) \ge n - 1 + (n - 2)(n - 4)/2 - n(n - 1)/6 = (2n^2 - 11n + 18)/6 > 0$.

Every term of the series in Equation (32) is therefore positive for $x > 0$ and $1 < r < 2$, and the right-hand side is zero for $r = 1$. Hence $\Lambda \ge \Lambda_2$, with equality if and only if $r = 1$, that is, $\varepsilon = 1/8$. Together with $\Lambda_2 \ge \Lambda_1$, this gives $\Lambda_1 \le \Lambda_2 \le \Lambda$. Because $\Lambda_1 > 0$ and the logarithm is strictly increasing, it follows that $\nu_{ref} \le \nu_2 \le \nu_1$ with equality in the same case. Rounding up to an integer preserves this order, so that $n_{ref} \le n_2 \le n_1$. □

No restriction on $N$ is needed in the proof, so the result holds for every resolution. For $P_3$, the first neglected coefficient of Equation (15), $A_4 = -s^4(2s-1)(48s^3-96s^2+32s+1)/45$, is positive for $1/2 < s < 1$, so that $\nu_3 \geq \nu_{ref}$ for sufficiently large $N$. The series argument of the proof does not extend to $P_3$, and for $N = 4$–$20$ the inequality is verified numerically in Section 5.2.

The proposition gives a sufficient condition for a conservative design count. In Equation (80) of [1], the integer design count over all code transitions is taken as $n_S = n_{ref} + 1$, where the additional period accounts for the decreasing transition. Since $n_{ref} \leq n_m$ for $m = 1$ and $m = 2$,

$$n_S = n_{ref} + 1 \leq n_m + 1, \qquad 1/8 \leq \varepsilon < 1/2, \qquad m = 1, 2, \tag{34}$$

for every $N$. One PWM period added to the rounded first-order or second-order count therefore gives a design count that is not smaller than that of [1], and a second period is not needed to compensate for the truncation. This result concerns the reference count, while the relation of $n_m + 1$ to the exact worst-case count over both transition directions is examined numerically in Section 5.4.

The one-period correction of [1] can be examined by applying the resolution expansion to the decreasing-transition expression, Equation (79) of [1], which gives

$$\nu_{\downarrow} - \nu_{ref} = \frac{2s-1}{2s} + O(\delta), \tag{35}$$

where $\nu_{\downarrow}$ denotes the continuous worst-case count of the decreasing transition. For $1/2 \leq s < 1$ the leading term lies between 0 and $1/2$. To leading order, the decreasing-transition count therefore exceeds the reference count by less than half a period, and the rounded counts differ by zero or one, in agreement with Table 1 of [1].

**Table 1.** Reference and truncated settling counts at the twelve operating points reported in [1] and four additional cases with $\varepsilon = 1/8$.

| $N$ | $\varepsilon$ | $\nu_{ref}$ | $n_{ref}$ | $P_1$ | $n_1$ | $P_2$ | $n_2$ | $P_3$ | $n_3$ |
|---|---|---|---|---|---|---|---|---|---|
| 6 | $\frac{1}{3}$ | 128.60 | 129 | 128.74 | 129 | 128.61 | 129 | 128.60 | 129 |
| 6 | $\frac{1}{4}$ | 161.19 | 162 | 161.29 | 162 | 161.19 | 162 | 161.19 | 162 |
| 6 | $\frac{1}{5}$ | 196.92 | 197 | 196.99 | 197 | 196.92 | 197 | 196.92 | 197 |
| 6 | $\frac{1}{8}$ | 310.53 | 311 | 310.53 | 311 | 310.53 | 311 | 310.53 | 311 |
| 8 | $\frac{1}{3}$ | 647.90 | 648 | 648.03 | 649 | 647.90 | 648 | 647.90 | 648 |
| 8 | $\frac{1}{4}$ | 822.50 | 823 | 822.60 | 823 | 822.50 | 823 | 822.50 | 823 |
| 8 | $\frac{1}{5}$ | 1009.70 | 1010 | 1009.77 | 1010 | 1009.70 | 1010 | 1009.70 | 1010 |
| 8 | $\frac{1}{8}$ | 1597.01 | 1598 | 1597.01 | 1598 | 1597.01 | 1598 | 1597.01 | 1598 |
| 10 | $\frac{1}{3}$ | 3124.32 | 3125 | 3124.45 | 3125 | 3124.32 | 3125 | 3124.32 | 3125 |
| 10 | $\frac{1}{4}$ | 4000.08 | 4001 | 4000.18 | 4001 | 4000.08 | 4001 | 4000.08 | 4001 |
| 10 | $\frac{1}{5}$ | 4926.25 | 4927 | 4926.32 | 4927 | 4926.25 | 4927 | 4926.25 | 4927 |
| 10 | $\frac{1}{8}$ | 7807.61 | 7808 | 7807.61 | 7808 | 7807.61 | 7808 | 7807.61 | 7808 |
| 12 | $\frac{1}{3}$ | 14,627.004 | 14,628 | 14,627.13 | 14,628 | 14,627.005 | 14,628 | 14,627.004 | 14,628 |
| 12 | $\frac{1}{4}$ | 18,839.74 | 18,840 | 18,839.84 | 18,840 | 18,839.74 | 18,840 | 18,839.74 | 18,840 |
| 12 | $\frac{1}{5}$ | 23,254.14 | 23,255 | 23,254.21 | 23,255 | 23,254.14 | 23,255 | 23,254.14 | 23,255 |
| 12 | $\frac{1}{8}$ | 36,908.70 | 36,909 | 36,908.70 | 36,909 | 36,908.70 | 36,909 | 36,908.70 | 36,909 |

## 5. Numerical Verification

The three truncations are compared with the reference criterion at the operating points reported in [1] and over an extended grid of $N$ and $\varepsilon$ values. The extended grid is also used

to examine how the truncation error changes with resolution. The reference expression and the truncations are then compared with the exact first-order model.

### *5.1. Operating Points*

Table 1 includes the twelve operating points reported in [1] and four additional cases with $\varepsilon = 1/8$, the lower limit of the considered range, where Equation (25) shows that the first-order approximation gives the same value as the reference expression. For the twelve operating points taken from [1], rounding $\nu_{ref}$ to $n_{ref}$ gives the same rising-transition counts as those published in [1].

Across Table 1, $P_1$ differs from the rounded reference count in only one case, at $N = 8$ and $\varepsilon = 1/3$, where $n_1 = 649$ and $n_{ref} = 648$. $P_2$ and $P_3$ give the same rounded count as the reference expression in all cases. For $\varepsilon = 1/8$, all three approximations give the same continuous count as the reference expression for $N = 6$, 8, 10 and 12, as predicted by Equation (25).

### *5.2. Extended Grid*

The extended grid uses $N = 4$–20 and $\varepsilon = 0.125$–0.45 in steps of 0.005, giving 1122 combinations. All quantities were calculated with fifty significant digits because $\Lambda$ is obtained as the difference in two nearly equal quantities. The coefficients in Equations (16)–(18) were also verified using the same calculation. The results are summarized in Table 2.

**Table 2.** Comparison of the three approximations with the reference expression over the extended grid of 1122 combinations.

| Truncation Order | Continuous Error [Periods] | Error Scaling | Matching Rounded Count [%] | Matching Cases | Maximum Integer Deviation |
|---|---|---|---|---|---|
| $P_1$ | $[0, +2.052 \cdot 10^{-1}]$ | $O(1)$ | 89.66% | 1006/1122 | 1 |
| $P_2$ | $[0, +5.027 \cdot 10^{-2}]$ | $O(2^{-N})$ | 99.82% | 1120/1122 | 1 |
| $P_3$ | $[0, +2.494 \cdot 10^{-3}]$ | $O(4^{-N})$ | 100.00% | 1122/1122 | 0 |

The continuous error gives the difference between each approximation and the reference expression before rounding, while the "error scaling" column shows how this error changes with the resolution $N$, as given by Equations (21)–(23). The columns "matching rounded count" and "matching cases" show the percentage and number of combinations for which the rounded approximation is equal to the rounded reference count. Finally, the "maximum integer deviation" column gives the largest difference between these rounded counts. Because the ceiling operation is applied to the continuous counts, even a small continuous error can produce a one-period difference in the integer count.

The error of $P_1$ never exceeds 0.21 periods over the grid, while the rounded count differs from the rounded reference count in 116 of the 1122 combinations, always by exactly one period upward. For $P_2$, the maximum error is 0.050 periods, and the rounded count differs from the rounded reference count at only two combinations, $N = 4$, $\varepsilon = 0.405$ and $N = 4$, $\varepsilon = 0.425$. For $P_3$, the maximum error is 0.0025 periods. Although the continuous error is not zero, the rounded count is equal to the rounded reference count for all 1122 combinations.

The errors of all three truncations are zero at the 17 combinations with $\varepsilon = 1/8$ and positive at the remaining 1105, so that no truncation lies below the reference count anywhere on the grid. For $P_1$ and $P_2$ this follows from the proposition in Section 4.4. For $P_3$ it is a numerical observation. Since the continuous errors are non-negative and remain below one

period on the extended grid, the rounded approximation exceeds the rounded reference count by at most one period.

### *5.3. Error Dependence on Resolution and Tolerance*

Figure 1 shows the maximum absolute continuous error over $\varepsilon = 0.125$–$0.45$ as a function of the resolution $N$. The three curves behave differently because $\Lambda$ is truncated at different orders in $\delta$. The first term omitted from $\Lambda_1$ is $A_2\delta^2$. Since both $\Lambda_1$ and $k$ are proportional to $\delta$, the leading error of $P_1$ is independent of $N$, as given by Equation (21). Retaining one or two additional terms reduces the leading errors to $O(\delta)$ and $O(\delta^2)$, respectively, in accordance with Equations (22) and (23). The errors of $P_2$ and $P_3$ therefore decrease approximately by factors of two and four per additional bit. On the logarithmic vertical scale of Figure 1 they form approximately straight lines whose slopes are in the ratio 1 to 2. The slight decrease in the $P_1$ error between $N = 4$ and $N = 8$, from 0.205 to 0.161, results from the $O(\delta)$ term of Equation (29).

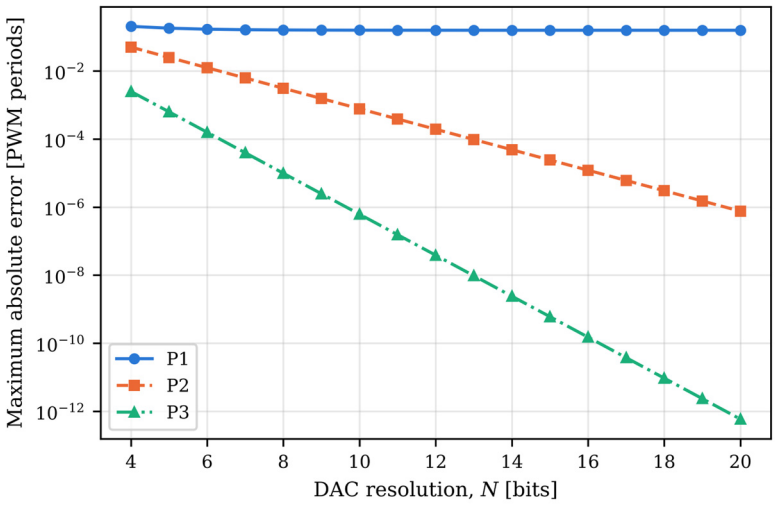



**Figure 1.** Maximum absolute continuous settling-count error over $\varepsilon = 0.125$–$0.45$ as a function of the DAC resolution $N$. The $P_1$ error approaches a value nearly independent of $N$, while the $P_2$ and $P_3$ errors decrease approximately as $2^{-N}$ and $4^{-N}$, respectively.

Figure 2 compares the $P_1$ error with the leading term $(2s - 1)/(6s)$ of Equation (21) for $N = 4, 8, 12$ and 20. Because $s = \sqrt{2\varepsilon}$, this term is a function of the tolerance only and is drawn as one solid curve for all resolutions. For $N = 8, 12$ and 20 the computed points lie on this curve. The largest visible difference occurs at $N = 4$, where the neglected higher-order term is largest. The separation of the $N = 4$ points from the leading-term curve increases gradually with the tolerance and becomes clearly visible in Figure 2 above $\varepsilon \approx 0.3$. It is caused by the $O(\delta)$ term of Equation (29) and does not indicate a change in the behavior of the converter. The coefficient of this term contains the factor $1/(1 - s)$ and increases as $\varepsilon$ approaches $1/2$, but it is multiplied by $\delta = 1/16$ for $N = 4$ and by $1/256$ or less for $N \geq 8$. For $N = 4$ the term equals 0.002 at $\varepsilon = 0.2$, 0.007 at $\varepsilon = 0.3$, and 0.047 at $\varepsilon = 0.45$. The dashed curve in Figure 2, which is the sum of the leading term and this term, closely follows the $N = 4$ points. Both curves start from zero at $\varepsilon = 1/8$, where Equation (25) gives a zero error for every resolution.

Figure 3 shows the errors of the three truncations near the upper limit $\varepsilon = 1/2$ as a function of the distance $1/2 - \varepsilon$ for $N = 4, 8$ and 12. Over the grid of Table 2 the left-hand side of Equation (28) does not exceed 0.013, a value reached at $N = 4$ and $\varepsilon = 0.45$. In the shaded area of Figure 3, which covers the tolerances of this grid, the errors remain within the ranges of Table 2. To the right of this area, closer to the limit, the $P_1$ and $P_2$

errors increase and merge. These two errors reach one period at $1/2 - \varepsilon = 0.0029$ and 0.0023, respectively, for $N = 4$, and at $1.9{\cdot}10^{-4}$ and $1.6{\cdot}10^{-4}$ for $N = 8$, in agreement with Equation (30). The $P_3$ error remains below 0.26 periods for all three resolutions.

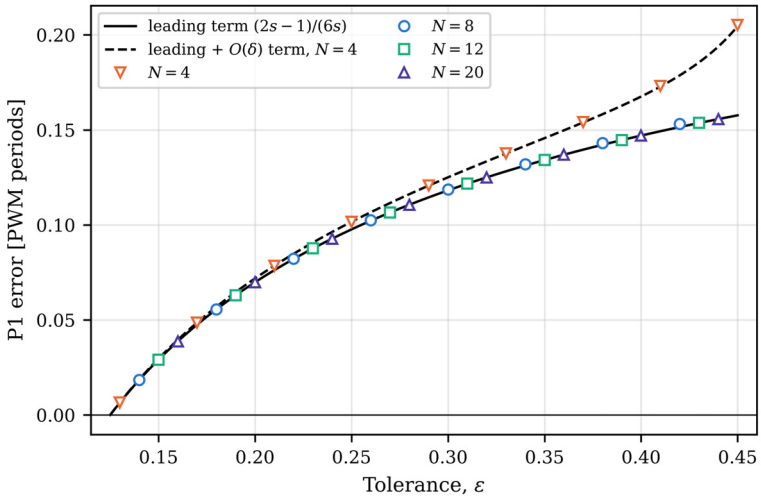



**Figure 2.** Error of $P_1$ as a function of the tolerance $\varepsilon$ for $N = 4$, 8, 12 and 20. The markers are the computed errors, and the four resolutions are marked at different tolerances of the grid so that the markers do not overlap. The solid line is the leading term $(2s - 1)/(6s)$ of Equation (21), where $s = \sqrt{2\varepsilon}$, and the dashed line is the sum of this term and the $O(\delta)$ term of Equation (29) for $N = 4$. All errors are zero at $\varepsilon = 1/8$ and positive above it.

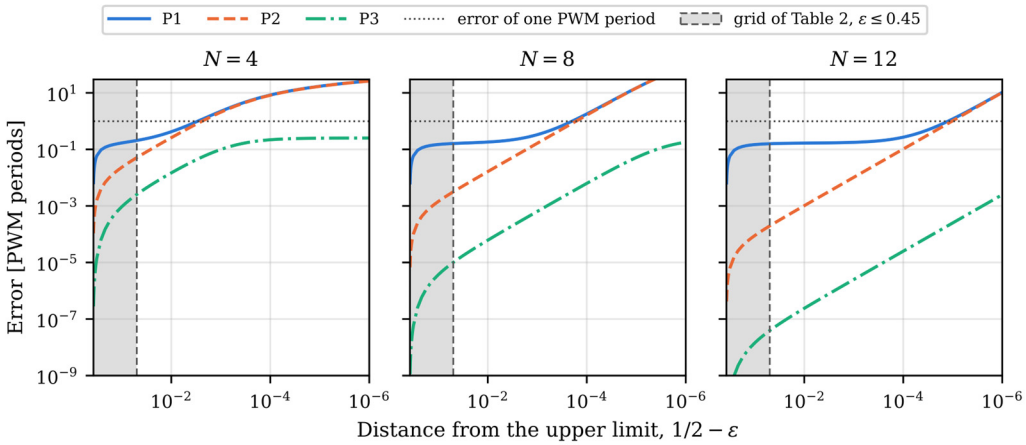



**Figure 3.** Errors of $P_1$, $P_2$, and $P_3$ relative to the reference expression near the upper limit $\varepsilon = 1/2$, for $N = 4, 8$ and 12. The horizontal axis shows the distance $1/2 - \varepsilon$ on a logarithmic scale, and the tolerance $\varepsilon$ increases from left to right. The dotted horizontal line marks an error of one PWM period. The shaded area covers the tolerances of the grid in Table 2, and the dashed vertical line at its right edge marks $\varepsilon = 0.45$, the largest tolerance of this grid.

The numerical results in Figures 1–3 follow the error behavior predicted by Equations (21)–(23) and Equations (28)–(30) over the tested range of $N$ and $\varepsilon$ values.

### *5.4. Comparison with the Exact First-Order Model*

The errors in Sections 5.1–5.3 are measured relative to $\nu_{ref}$. To separate the truncation error from the approximations contained in $\nu_{ref}$, the exact count $\nu_{ex}$ defined in Section 2 was evaluated. The position of the maximum for a continuous target code is the solution of Equation (66) of [1]. In [1] this equation was solved approximately, which gives Equation (3), while here it is solved exactly with the Lambert W function [11]. The filter parameter is kept at its design value given by Equation (2), so that only the approximation of the

position of the maximum is removed. The exact count was then taken as the largest value of Equation (65) of [1] at the admissible integer codes adjacent to this position, and the highest code was used when the position lies above the code range. The integer target code at which this largest value is reached is denoted by $d_{2,ex}$. For $N = 4 - 8$ the result was confirmed by evaluating all admissible target codes. The total error of a truncation is

$$\nu_m - \nu_{ex} = (\nu_m - \nu_{ref}) + (\nu_{ref} - \nu_{ex}), \tag{36}$$

where the first term is the truncation error introduced in the present work and the second is inherited from the reference expression. Table 3 lists the second term and the total errors of the three truncations at the twelve operating points of [1].

**Table 3.** Comparison with the exact first-order model at the twelve operating points reported in [1]. The columns give the worst-case integer target code $d_{2,ex}$, the exact count $\nu_{ex}$, and the differences $\nu_{ref} - \nu_{ex}$ and $\nu_m - \nu_{ex}$ ($m = 1, 2, 3$) in units of $10^{-3}$ PWM periods. In all rows $n_{ref} = n_2 = n_3 = n_{ex}$.

| $N$ | $\varepsilon$ | $d_{2,ex}$ | $\nu_{ex}$ | $\nu_{ref} - \nu_{ex}$ [$10^{-3}$] | $\nu_1 - \nu_{ex}$ [$10^{-3}$] | $\nu_2 - \nu_{ex}$ [$10^{-3}$] | $\nu_3 - \nu_{ex}$ [$10^{-3}$] | $n_{ex}$ | $n_1$ |
|---|---|---|---|---|---|---|---|---|---|
| 6 | $\frac{1}{3}$ | 39 | 128.5998 | 4.34 | 135.97 | 7.11 | 4.36 | 129 | 129 |
| 6 | $\frac{1}{4}$ | 45 | 161.1855 | 4.04 | 102.67 | 5.18 | 4.04 | 162 | 162 |
| 6 | $\frac{1}{5}$ | 51 | 196.9208 | 0.58 | 70.89 | 1.15 | 0.59 | 197 | 197 |
| 8 | $\frac{1}{3}$ | 157 | 647.8978 | −0.25 | 129.56 | 0.44 | −0.25 | 648 | 649 |
| 8 | $\frac{1}{4}$ | 181 | 822.5006 | 0.05 | 97.93 | 0.33 | 0.05 | 823 | 823 |
| 8 | $\frac{1}{5}$ | 203 | 1009.7030 | 0.91 | 70.85 | 1.05 | 0.91 | 1010 | 1010 |
| 10 | $\frac{1}{3}$ | 627 | 3124.3170 | 0.07 | 129.43 | 0.25 | 0.07 | 3125 | 3125 |
| 10 | $\frac{1}{4}$ | 724 | 4000.0791 | 0.05 | 97.75 | 0.12 | 0.05 | 4001 | 4001 |
| 10 | $\frac{1}{5}$ | 810 | 4926.2539 | 0.07 | 69.92 | 0.11 | 0.07 | 4927 | 4927 |
| 12 | $\frac{1}{3}$ | 2508 | 14,627.0044 | 0.11 | 129.36 | 0.16 | 0.11 | 14,628 | 14,628 |
| 12 | $\frac{1}{4}$ | 2896 | 18,839.7405 | 0.08 | 97.73 | 0.10 | 0.08 | 18,840 | 18,840 |
| 12 | $\frac{1}{5}$ | 3238 | 23,254.1390 | 0.03 | 69.85 | 0.04 | 0.03 | 23,255 | 23,255 |

At the twelve operating points the difference between the reference count and the exact count lies between $-2.5{\cdot}10^{-4}$ and $4.3{\cdot}10^{-3}$ PWM periods, and the rounded counts are equal in every case. At each operating point the code $d_{2,ex}$ is one of the two integers adjacent to the position given by Equation (3). For $N = 8$ and $\varepsilon = 1/4$ it equals 181, which is the target code of the transition used in the simulations and measurements of [1]. The difference between the reference count and the exact count is at least an order of magnitude smaller than the truncation error of $P_1$ and is comparable to that of $P_2$ at $N = 6$. For $P_3$ the truncation error is smaller in magnitude than this difference at every point, and the accuracy of $P_3$ relative to the exact model is therefore limited by the reference expression. $P_2$ and $P_3$ reproduce the rounded exact count at all twelve points, while $P_1$ reproduces it at eleven points and differs only at $N = 8$, $\varepsilon = 1/3$, as in Table 1.

Over the extended grid, $\nu_{ref} - \nu_{ex}$ lies between approximately $-0.0097$ and 0.089 PWM periods, and the largest value occurs at $N = 4$ and $\varepsilon = 1/8$. Since $n_{ref} = n_{ex}$ at all 1122 combinations, the rounded-count agreement in Table 2 also holds with respect to the exact model, and no truncation gives a rounded count smaller than the rounded exact count. The total errors relative to the exact model do not exceed 0.28, 0.12, and 0.089 PWM periods for $P_1$, $P_2$, and $P_3$, respectively.

The exact worst-case count of the decreasing transition was obtained by maximizing Equation (75) of [1] over the integer target codes. Its rounded value equals $n_{ref}$ or $n_{ref} + 1$ at every combination, in agreement with Equation (35). The exact worst-case count over both transition directions therefore does not exceed $n_1 + 1$, $n_2 + 1$, or $n_3 + 1$ at any of the

1122 combinations. This is a numerical result for the tested grid, and a general proof with respect to the exact model is not given.

## 6. Discussion

The first-order approximation $P_1$ provides the simplest form of the rising-transition reference expression. Equation (20) contains no exponential terms and shows the dependence on $N$ and $\varepsilon$ directly. Its leading error depends only on $\varepsilon$ and is zero at $\varepsilon = 1/8$, where $P_1$ is equal to the reference expression for every resolution $N$. On the tested grid, the continuous error is below 0.21 PWM periods, although rounding can change the integer count by one period.

In practical design, $P_1$ serves as an analytical estimate. At fixed tolerance, Equation (20) shows that the count grows approximately as $N2^N$. The rounded count of $P_1$ differs from the rounded reference count at 116 of the 1122 tested combinations (10.3%). At all of them the deviation is one period upward, which is the direction that follows from the proposition in Section 4.4. $P_1$ therefore does not underestimate the reference count, but it is not exact after rounding. When the integer settling count is required, $P_2$ or $P_3$ should be used, at the additional cost of one or two algebraic terms in Equation (19).

The second-order and third-order approximations reduce the error by including additional terms of the expansion. The error of $P_2$ decreases with resolution as $2^{-N}$, while the error of $P_3$ decreases as $4^{-N}$, in accordance with Equations (22) and (23). The numerical results in Section 5 show that $P_2$ differs from the rounded reference count at only two combinations, both for $N = 4$, while $P_3$ gives the same rounded count as the reference expression for all tested combinations. Neither lies below the reference count on the grid, which follows from the proposition for $P_2$ and is a numerical observation for $P_3$.

The results are given for the considered range $1/8 \leq \varepsilon < 1/2$, because below $1/8$ the reference expression is evaluated at a position above the code range and overestimates the exact count. Close to $1/2$, at the distance estimated by Equation (30), the errors of the first-order and second-order truncations reach one period. The comparison with the exact first-order model shows that the accuracy of $P_3$ is limited by the reference expression. The truncation error of $P_3$ is below 0.0025 periods, while the reference count differs from the exact count by up to 0.089 periods at $N = 4$. Further terms would reduce the truncation error relative to the reference expression, but would not remove the error inherited from that expression. The analysis uses the ideal first-order model of [1]. Component tolerances, which are examined in [1], are outside its scope.

## 7. Conclusions

This work derives a resolution expansion of the rising-transition settling-time expression of [1] in $\delta = 2^{-N}$, with the tolerance $\varepsilon$ retained exactly. The first-order expression, Equation (20), removes the exponential quotient and shows the dependence on $N$ and $\varepsilon$ explicitly. Its leading error depends only on $\varepsilon$, and at $\varepsilon = 1/8$ the first-order expression coincides with the reference expression for every resolution. In Equation (26) it is written as the sum of two terms. The first is the number of periods in which an RC filter settles to within $\frac{1}{2}$LSB after a full-scale step, and the second is a correction that is zero at this tolerance.

The analysis is restricted to $1/8 \leq \varepsilon < 1/2$, because for smaller tolerances the position given by Equation (3) lies above the code range. For an arbitrary first-order RC filter, this interval corresponds to $2^{N-2} < RC/T \leq 2^N$, and near the lower limit of this ratio the first-order and second-order truncations lose accuracy.

Over the grid of 1122 combinations with $N = 4$–20 and $\varepsilon = 0.125$–0.45, the maximum continuous errors relative to the reference expression are 0.21, 0.050, and 0.0025 PWM

periods for $P_1$, $P_2$, and $P_3$, respectively. Their rounded counts agree with the rounded reference count at 1006, 1120, and 1122 combinations. At each point of this grid, the reference expression and the exact first-order model also yield the same rounded rising-transition count.

By the proposition in Section 4.4, $P_1$ and $P_2$ do not underestimate the reference count anywhere in the considered range, for every resolution. Adding one PWM period to either rounded count therefore gives a design count no smaller than that of [1]. For $P_3$, non-underestimation of the reference count is verified numerically over the tested grid only. For all three truncations, the same correction covers the exact worst-case count over both transition directions at all 1122 tested combinations. This agreement with the exact first-order model is a numerical finding for the tested grid, and the proposition does not establish a general bound relative to that model. $P_1$ is intended as an analytical estimate, and $P_2$ or $P_3$ should be used when the integer count is needed.

**Supplementary Materials:** The following supporting information can be downloaded at https://www.mdpi.com/article/10.3390/electronics15214910/s1, Supplementary File S1: Reproducibility package containing the Python 3.13 script that reproduces Tables 1–3 and Figures 1–3 and prints the numerical checks whose results are quoted in the text, together with the README.txt and requirements.txt files.

**Author Contributions:** Conceptualization, P.P. and V.R.; methodology, P.P. and V.R.; validation, D.Đ. and V.R.; formal analysis, P.P.; investigation, P.P.; resources, V.R.; data curation, P.P.; writing—original draft preparation, P.P.; writing—review and editing, D.Đ. and V.R.; visualization, P.P.; supervision, V.R.; project administration, V.R.; funding acquisition, P.P., D.Đ. and V.R. All authors have read and agreed to the published version of the manuscript.

**Funding:** This research was funded by the Vlatacom Institute of High Technologies under project #P161 vCCF155MM.

**Data Availability Statement:** The numerical data supporting the results presented in this study can be reproduced using the Python script provided in the Supplementary Materials. The script generates the data used for Tables 1–3 and Figures 1–3. No external datasets were used in this study.

**Acknowledgments:** This work was financially supported by the Ministry of Science, Technological Development, and Innovation of the Republic of Serbia under contract number 451-03-34/2026-03/200103. During the preparation of this manuscript and the accompanying Python script, the authors used ChatGPT (GPT-5.6 Sol, OpenAI) for assistance with script organization and language and formatting of the manuscript text. The authors reviewed and verified the Python script and the manuscript content and take full responsibility for the content of this publication.

**Conflicts of Interest:** The authors declare no conflicts of interest. The funders had no role in the design of the study; in the collection, analyses, or interpretation of data; in the writing of the manuscript; or in the decision to publish the results.

## Abbreviations

The following abbreviations are used in this manuscript:

| | |
|---|---|
| PWM | Pulse-Width Modulation |
| RC | Resistor–Capacitor |
| LSB | Least Significant Bit |
| DAC | Digital-to-Analog Converter |

## References

1. Petronijević, P.; Elez, J.; Đokić, D.; Rajović, V. Accuracy Optimization and Settling Time Characterization of an N-Bit PWM DAC with a First-Order RC Filter. *Electronics* **2026**, *15*, 2760. [CrossRef]

2. Elez, J.; Jakišić, N.; Đokić, D.; Rajović, V.; Popović Božović, J. Time-Domain Analysis of a PWM DAC with a First-Order Passive RC Filter. In Proceedings of the 32nd Telecommunications Forum (TELFOR), Belgrade, Serbia, 26–27 November 2024; pp. 352–355. [CrossRef]
3. Halper, C.; Heiss, M.; Brasseur, G. Digital-to-Analog Conversion by Pulse-Count Modulation Methods. *IEEE Trans. Instrum. Meas.* **1996**, *45*, 805–814. [CrossRef]
4. Zhou, F.; Xiong, W. Using PWM Output as a Digital-to-Analog Converter on DSP. In Proceedings of the 2010 International Conference on System Science, Engineering Design and Manufacturing Informatization, Yichang, China, 12–14 November 2010; pp. 278–281. [CrossRef]
5. Nneme Nneme, L.; Moffo Lonla, B.; Sonfack, G.B.; Mbihi, J. Review of a Multipurpose Duty-Cycle Modulation Technology in Electrical and Electronics Engineering. *J. Electr. Eng. Electron. Control Comput. Sci.* **2018**, *4*, 9–18.
6. Viegas, V.; Dias Pereira, J.M. Digital to Analog Converter Based on Pulse-Width Adding. *Meas. Sens.* **2025**, *38*, 101418. [CrossRef]
7. Gupta, R.; Tutuianu, B.; Pileggi, L.T. The Elmore Delay as a Bound for RC Trees with Generalized Input Signals. *IEEE Trans. Comput.-Aided Des. Integr. Circuits Syst.* **1997**, *16*, 95–104. [CrossRef]
8. Yang, H.C.; Allstot, D.J. Considerations for Fast Settling Operational Amplifiers. *IEEE Trans. Circuits Syst.* **1990**, *37*, 326–334. [CrossRef]
9. Middlebrook, R.D. Low-Entropy Expressions: The Key to Design-Oriented Analysis. In Proceedings of the Frontiers in Education Twenty-First Annual Conference, West Lafayette, IN, USA, 21–24 September 1991; pp. 399–403. [CrossRef]
10. Olver, F.W.J. *Asymptotics and Special Functions*; A K Peters: Wellesley, MA, USA, 1997. [CrossRef]
11. Corless, R.M.; Gonnet, G.H.; Hare, D.E.G.; Jeffrey, D.J.; Knuth, D.E. On the Lambert W Function. *Adv. Comput. Math.* **1996**, *5*, 329–359. [CrossRef]
12. Tsoulos, I.G.; Stavrou, V.; Mastorakis, N.E.; Tsalikakis, D. GenConstraint: A Programming Tool for Constraint Optimization Problems. *SoftwareX* **2019**, *10*, 100355. [CrossRef]
13. Chapman, C.J.; Wynn, H.P. Fractional Power Series and the Method of Dominant Balances. *Proc. R. Soc. A* **2021**, *477*, 20200646. [CrossRef]
14. Chapman, C.J.; Wynn, H.P.; Atherton, M.A.; Bates, R.A. Non-Dimensional Newton–Puiseux Expansions. *arXiv* **2021**, arXiv:2111.05762. [CrossRef]


**Disclaimer/Publisher's Note:** The statements, opinions and data contained in all publications are solely those of the individual author(s) and contributor(s) and not of MDPI and/or the editor(s). MDPI and/or the editor(s) disclaim responsibility for any injury to people or property resulting from any ideas, methods, instructions or products referred to in the content.